Chapter 24

Turbulence and heat flux formulations

24.1 Test case *pycno*

24.1.1 Theory

This test case is a 1-D problem describing the evolution of a wind-driven surface mixed layer in the absence of rotation. Although simple in form the problem is of considerable oceanographic interest. Moreover it allows to intercompare in a simple way the different turbulence formulations implemented in the program. The initial state consists of a water column at rest with a stable stratification in the vertical using a constant density gradient. A surface stress is applied initially remaining uniform in space and time. A surface mixed layer develops which grows in time. The deepening is governed by the entrainment of denser water at the base of the mixed layer. As will be shown below the process critically depends on some parameters of the turbulence formulation while others are of less importance.

The basic equations in the absence of advection and horizontal diffusion are given by

$$\frac{\partial u}{\partial t} = \frac{\partial}{\partial z}\left(\nu_T \frac{\partial u}{\partial z}\right) \tag{24.1}$$

$$\frac{\partial \rho}{\partial t} = \frac{\partial}{\partial z}\left(\lambda_T \frac{\partial \rho}{\partial z}\right) \tag{24.2}$$

where z is the vertical coordinate (increasing upwards and zero at the surface), u the current, ρ the density and ν_T, λ_T the vertical eddy coefficients[1].

[1]The eddy coefficients reduce to their molecular values in the absence of turbulence.

The initial and boundary conditions are given by

$$u = 0 \ , \ -\frac{g}{\rho}\frac{\partial \rho}{\partial z} = N_0^2 \quad \text{at} \quad t = 0 \tag{24.3}$$

$$\nu_T \frac{\partial u}{\partial z} = u_{*s}^2 \ , \ \lambda_T \frac{\partial \rho}{\partial z} = 0 \quad \text{at} \quad z = 0 \tag{24.4}$$

where N_0 is the uniform initial buoyancy frequency and ρ_0 a reference density.

Kundu (1981) explored the possibility to cast the solutions of (24.1) and (24.2) into a self-similar form

$$u(z,t) = \hat{U}(t)F(\xi) \tag{24.5}$$

$$\rho(z,t) = \rho_h(t) + (\hat{\rho}(t) - \rho_h(t))G(\xi) \tag{24.6}$$

where $\xi = -z/h(t)$, $h(t)$ is the depth of the turbulent layer[2], ρ_h the density at the base of the layer and $\hat{U}, \hat{\rho}$ the values of respectively the current and density averaged over the turbulent layer. He showed that (24.5)–(24.6) are acceptable forms provided that the following additional assumptions are made:

- $u = 0$ and $Ri = -\rho_0(\partial u/\partial z)^2/(g(\partial \rho/\partial z)) = Ri_c$ at $z = -h$ where Ri_c is a constant critical Richardson number
- the eddy coefficients can be cast into the form

$$\nu_T = f_\nu(\xi)h^2/t \ , \ \lambda_T = f_\lambda(\xi)h^2/t \tag{24.7}$$

The solutions of (24.1)–(24.2) can then be written as

$$u(z,t) = \frac{u_{*s}}{(2\overline{Ri})^{1/4}}F(\xi)(tN_0)^{1/2} \tag{24.8}$$

$$\begin{aligned} \Delta\rho(z,t) &= \rho(z,t) - \rho(z,0) \\ &= \frac{\rho_0 N_0^2}{2g}(2 - 2\xi - G(\xi))h(t) \end{aligned} \tag{24.9}$$

and

$$h(t) = (2\overline{Ri})^{1/4}u_{*s}(t/N_0)^{1/2} \tag{24.10}$$

The bulk Richardson number $\overline{Ri}$ is defined by

$$\overline{Ri} = \frac{N_0^2 h^2(t)}{2\hat{U}^2(t)} = -\frac{F'^2(1)}{G'(1)}Ri_c = \text{constant} \tag{24.11}$$

where a $'$ denotes a derivative with respect to ξ. For a more profound theoretical discussion of this idealised mixed layer problem the reader is referred to the papers by e.g. Kundu (1981); Kranenburg (1983); Luyten *et al.* (1996).

[2]This definition of h should not be confused with the one for the mean water depth.

24.1.2 Model setup

Equations (24.1)–(24.4) are solved numerically with the following parameters

$$u_{*s} = 0.01\text{m/s} \ , \ N_0 = 0.01\text{s}^{-1} \tag{24.12}$$

for a simulated period of 1 day. The total water depth is set to 100 m which is more than 2 times larger than the simulated mixed layer depths. The density equation (24.2) is transformed into an equivalent salinity equation using a linear equation of state. The initial salinity field is given by

$$S = S_0 - \frac{N_0^2}{g\beta_S}(z + H) \tag{24.13}$$

where S_0 is a reference salinity and H the water depth.

24.1.3 Experiments and output parameters

Seven numerical experiments have been defined by setting a number of turbulence switches. The following schemes are used in the experiments:

A **:** zero-equation $k - l$ model using the Mellor-Yamada expressions for the stability functions and the "Blackadar" mixing length formulation (4.216)–(4.217)

B **:** one-equation model using the Munk-Anderson formulation (4.199) for the stability functions and the "Blackadar" mixing length (4.216)–(4.217) without limiting conditions

C **:** as scheme ***B*** now including the limiting conditions (4.225)–(4.226)

D **:** one-equation model using the $k - \varepsilon$ and Hossain-Rodi formulation for the stability functions, and the parabolic mixing length (4.213) with limiting conditions enabled

E **:** as scheme ***D*** now using Blackadar's (4.216)–(4.217) mixing length formulation

F **:** two-equation $k - l$ model using the Mellor-Yamada formulation for the stability functions and with limiting conditions enabled

G **:** two-equation $k - \varepsilon$ model using the Hossain-Rodi formulation for the stability functions and with limiting conditions enabled.

Table 24.1: Settings of the turbulence switches for the ***pycno*** experiments. A "-" means that the value of the switch is irrelevant.

switch	***A***	***B***	***C***	***D***	***E***	***F***	***G***
iopt_turb_ntrans	0	1	1	1	1	2	2
iopt_turb_param	1	1	1	2	2	1	2
iopt_turb_stab_form	3	2	2	3	3	3	3
iopt_turb_lmix	4	4	4	1	4	-	-
iopt_turb_stab_mod	1	-	1	4	4	1	4
iopt_turb_iwlim	0	0	1	1	1	1	1

Values of the corresponding turbulence switches are listed in Table 24.1. Note that experiment ***E*** corresponds to the default scheme of the program (except for the inclusion of limiting conditions). All schemes, except ***B*** and ***C***, yield a critical Richardson number so that the first criterion for self-similarity is satisfied. It can be demonstrated that none of the schemes complies with the second criterion. As shown by Luyten *et al.* (1996) the latter condition is of minor importance.

Time series of the mixed layer depth $h(t)$, the surface current $u(0,t)$ and the surface density difference $\Delta\rho(0,t)$ are shown in Figures 24.1a–f. The mixed layer depth is determined as the surface distance of the first grid point below the surface where the current is lower than 1% of its surface value. Vertical profiles of the current u, the density ρ minus the initial surface value $\rho(0,0)$ and the Richardson number at the end of the simulation period are plotted in Figure 24.2.

A number of output parameters are defined. Their intention is primarily to compare the results with the self-similarity theory. Equations (24.8)–(24.11) for the surface current, the surface value of $\Delta\rho$, $h(t)$ and $\overline{Ri}$ are then written in the form

$$\ln h = \alpha_h + \beta_h \ln(tN_0) \tag{24.14}$$

$$\ln u(0,t) = \alpha_u + \beta_u \ln(tN_0) \tag{24.15}$$

$$\ln \Delta\rho(0,t) = \alpha_d + \beta_d \ln(tN_0) \tag{24.16}$$

$$\ln \overline{Ri} = \alpha_r + \beta_r \ln(tN_0) \tag{24.17}$$

where, according to the self-similarity theory,

$$\beta_h = \beta_u = \beta_d = 1/2 \ , \ \beta_r = 0 \tag{24.18}$$

and

$$\alpha_h = \frac{1}{4}\ln(2\overline{Ri}) + \ln\Big(\frac{u_{\star s}}{N_0}\Big) \tag{24.19}$$

The eight coefficients (α_h,α_u,α_d,α_r), (β_h,β_u,β_d,β_r) in (24.14)–(24.17) are determined from the model results by applying a linear regression analysis. To remove the influence of initial conditions and adjustments the analysis is restricted to the last 14 hours. A description of all output parameters is given below.

rvmean The value of $\overline{Ri}$ defined by (24.11) and averaged over the last 14 hours.

brv The coefficient β_r in the linear relation (24.17) for $\overline{Ri}$.

corrv The squared correlation coefficient r^2 for the linear relation (24.17). A zero value indicates that $\overline{Ri}$ is uncorrelated with time.

rvmean2 The value of $\overline{Ri}$ as determined from (24.19).

bh The coefficient β_h in the linear relation (24.14) for $h(t)$ (log(m)).

corrh The squared correlation coefficient r^2 for the linear relation (24.14).

bu2 The coefficient β_u in the linear relation (24.15) for $u(0,t)$ (log(m/s)).

corru2 The squared correlation coefficient r^2 for the linear relation (24.15).

bdr0 The coefficient β_d in the linear relation (24.16) for $\Delta\rho(0,t)$ (log(kg/m^3)).

corrdr0 The squared correlation coefficient r^2 for the linear relation (24.16).

vedmax The maximum value of the eddy viscosity coefficient ν_T over the whole water depth (m^2/s) at the end of the simulation.

difmax The maximum value of the eddy diffusion coefficient λ_T over the whole water depth (m^2/s) at the end of the simulation.

tkemax The maximum value of the turbulence energy k over the whole water depth (J/kg) at the end of the simulation .

tmld The value of h at the end of the simulation (m).

usur The value of the surface velocity at the end of the simulation (m/s).

drosur The value of the surface density difference $\Delta\rho$ at the end of the simulation (kg/m^3).

sdev The relative difference between the depth-averaged salinity and its initial value, defined by

$$\mathsf{sdev} = 10^5(\overline{S}(t) - \overline{S}(0))/\overline{S}(0) \tag{24.20}$$

where an overbar denotes a depth-averaged value. Since there are no bottom and surface salinity fluxes, the exact value of sdev is zero. A conservative scheme is applied in the model for the vertical diffusion of salinity so that non-zero values are only due to rounding errors. This parameter is therefore useful to test the machine accuracy.

Values for all experiments are given in Table 24.2.

Table 24.2: Output values for the parameters of test case ***pycno***.

parameter	***A***	***B***	***C***	***D***	***E***	***F***	***G***
rvmean	0.3318	4.028	1.014	0.6097	0.5974	0.6002	0.4777
brv	0.0592	0.3793	0.0503	0.0357	0.0176	0.0361	-0.0529
corrv	0.2223	0.9702	0.3253	0.1602	0.0568	0.2012	0.0036
rvmean2	0.2275	0.3559	0.7355	0.4852	0.5341	0.4766	0.4942
bh	0.5147	0.5948	0.5126	0.5089	0.5044	0.5090	0.4987
corrh	0.9971	0.9992	0.9987	0.9984	0.9987	0.9987	0.9980
bu2	0.5019	0.3515	0.4106	0.4294	0.4267	0.4159	0.4214
corru2	0.9999	0.9997	1.000	1.000	1.000	1.000	0.9999
bdro	0.4897	0.5653	0.5356	0.5254	0.5303	0.5329	0.5374
corrdro	0.9999	1.000	1.000	1.000	1.000	1.000	1.000
vedmax	10.19	1.247	1.187	1.890	1.252	1.506	1.350
difmax	12.79	1.422	1.385	2.587	1.825	2.166	1.663
tkemax	226.2	3.254	3.254	3.036	3.036	3.036	4.362
tmld	26.75	51.25	35.25	30.75	30.75	30.75	29.25
usur	0.6497	0.4002	0.4377	0.4415	0.4634	0.4518	0.4789
drosur	0.0987	0.1530	0.1418	0.1348	0.1333	0.1340	0.1244
sdev	-2.337	-4.297	-13.01	-0.1192	-0.0596	-0.0954	-0.9775

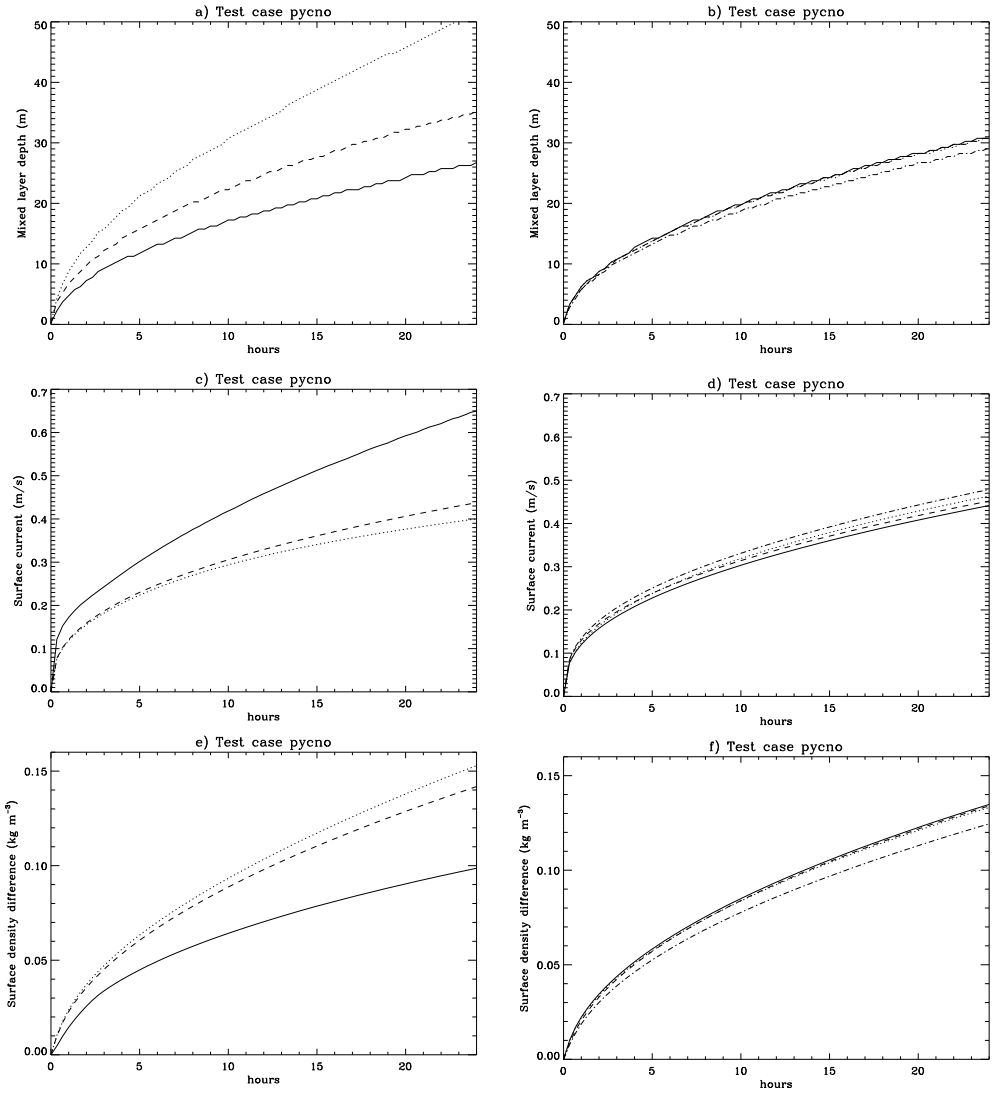

Figure 24.1: Test case ***pycno***. Time series of the mixed layer depth (a–b), the surface current (c–d) and the surface density difference $\Delta\rho(0,t)$ (e–f). Test runs ***A, B, C***, are represented in Figures a, c, e by the solid, dotted and dashed curves respectively. Test runs ***D, E, F, G*** are shown in Figures b, d, f by the solid, dotted, dashed and dash-dotted curves respectively.

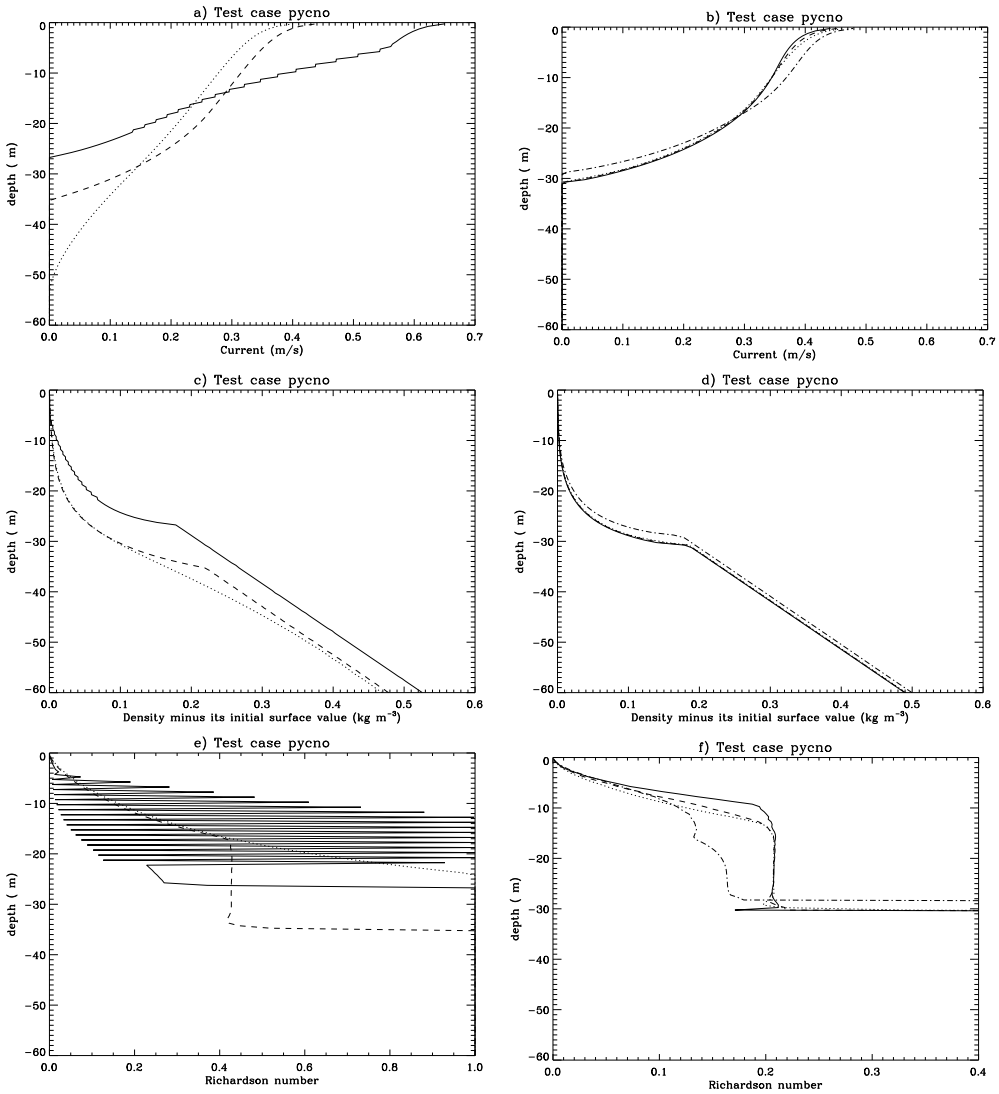

Figure 24.2: Test case ***pycno***. Vertical profiles of the current (a–b), the density minus its initial surface value, $\rho(z,t) - \rho(0,0)$ (c–d) and the Richardson number (e–f) after one day. Experiments ***A, B, C*** are represented in (a), (c), (e) by the solid, dotted and dashed-dotted curves respectively. Experiments ***D, E, F, G*** are shown in (b), (d), (f) by the solid, dotted, dashed and dash-dotted curves respectively.

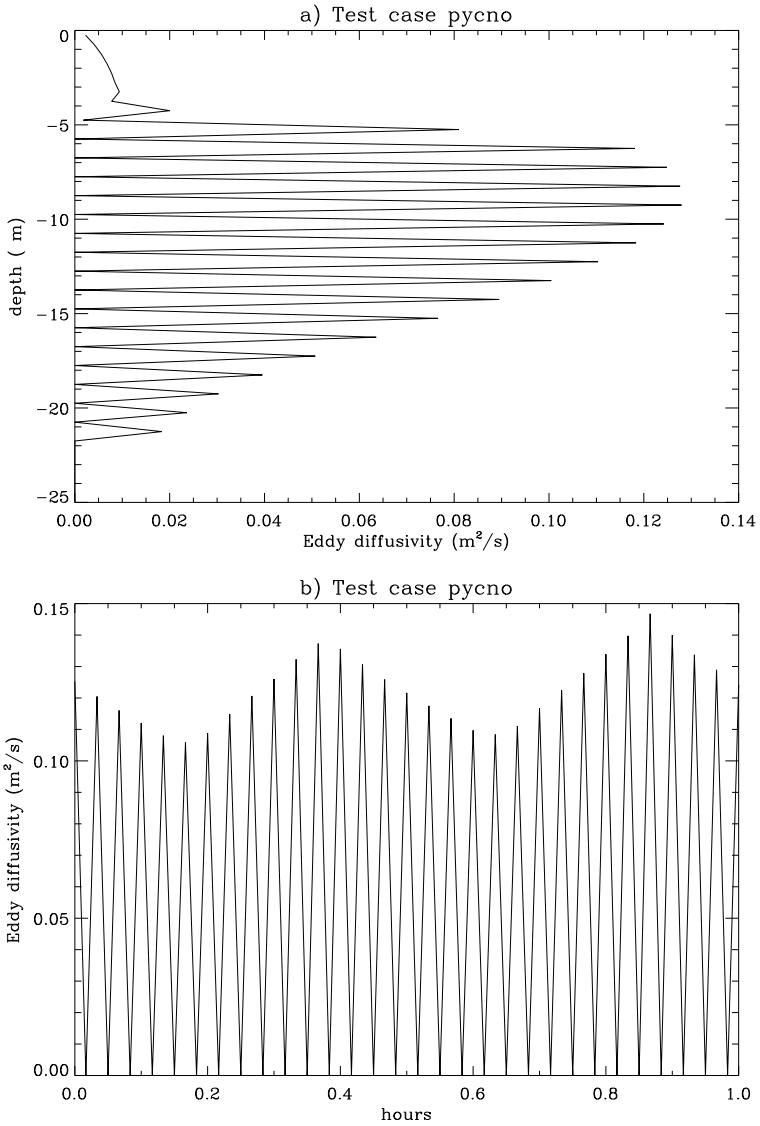

Figure 24.3: Test case ***pycno***. Vertical profile of the vertical diffusion coefficient λ_T after one day (a) and time series of λ_T at 10 m depth during the last hour of the simulation (b) for experiment ***A***.

24.1.4 Results

The results can be summarised as follows:

- The time-averaged bulk Richardson number $\overline{Ri}$ (parameter rvmean) is much higher for the schemes ***B*** and ***C*** which use the Munk-Anderson formulation for the stability functions compared to the other schemes using a RANS model.

- The general time dependence of $\overline{Ri}$ (not shown) consists of an oscillation around a mean value which increases in time. The amplitude of the oscillations and the growth rate of the mean value of $\overline{Ri}$ remain small in all cases except ***B***. This explains why brv is larger for ***B*** compared to the other experiments.

- The parameter rvmean2 is mostly lower than rvmean. The former is obtained from the linear regression analysis and (24.19) whereas the latter is evaluated using its definition (24.11). The difference is larger for the schemes ***A***−***C*** indicating that the self-similarity hypothesis is less valid for this type of schemes. The laboratory data of Kato & Phillips (1969) calibrated by Price (1979) yield a value of $\overline{Ri}$ close to 0.6 which agrees more with the values predicted by the RANS schemes ***D, E, F, G*** than the ones obtained from the Munk-Anderson formulations ***B, C***.

- The parameters β_h and β_d are close to 0.5 in agreement with the value predicted by the self-similarity theory whereas $\beta_u \simeq 0.4$ (except for case ***A***) which is lower than the theoretical value of 0.5.

- For larger values of $\overline{Ri}$ (parameter rvmean) the surface current tends to decrease whereas the surface density and the mixed layer depth tend to increase in agreement with equations (24.8)–(24.10).

- The schemes ***D*** to ***G*** produce larger shears near the surface and much shallower mixed layer depths compared to the ***B*** and ***C*** schemes. Note the remarked difference between the zero-equation and two-equation models ***A*** and ***F*** which are physically nearly the same. The discrepancy is most clearly observed in the profiles of the current (Figures 24.2a–b and the density (Figures 24.2c–d).

- From Figures 24.2e–f one observes that the Richardson number approaches its critical value in the stratified zone just below the surface mixed layer (except in the runs ***A*** and ***B***). Note that $Ri \simeq Ri_c$ at the base of the turbulent layer for the schemes ***C***–***G*** which use a limiting

condition (iopt_turb_iwlim=1). The highly oscillating curve for run ***A*** is due to a numerical instability (see below).

- It is clear that the results obtained with the zero-equation model ***A*** should not be considered as realistic. This type of schemes becomes numerically unstable either when the time step Δt is too large or the vertical grid spacing Δz is too small. The problem is illustrated in Figures 24.3 showing the vertical profile of λ_T at the end of the simulation and a time series of λ_T for the last hour of the run at 10 m depth. An unrealistic "jittering" is observed oscillating over 2 vertical grid spacings. The problem can be remedied by increasing the vertical resolution. A more elaborate discussion can be found in Frey (1991); Luyten *et al.* (1996). Since there exists no clear criterion for the stability of the level 2 schemes, it is recommended to avoid the zero-equation scheme in a realistic model application.

24.2 Test case *csnsp*

24.2.1 Description of the problem and model setup

The intention of the previous test case is to verify the different turbulence schemes implemented in the program against analytical solutions. The setup of these applications is however far from the realistic conditions prevailing in coastal and shelf seas. A more realistic study should take account of the effects of e.g. wind, tides and seasonal stratification. Test case ***csnsp*** has been constructed for this purpose. This simulates the annual cycle of thermal stratification at station CS (55° 30′N, 0° 55′E) located in the deeper parts of the North Sea where a thermocline forms during the summer. The model is forced using realistic meteorological and tidal data. To limit CPU time the simulation is performed with the 1-D (water column) version of the program so that advective effects are ignored. The results can validated with the observed data sets of the UK North Sea Project (Charnock *et al.*, 1994). This test case allows to compare the influence of different formulations available in the program (turbulence, boundary conditions, optics, equation of state).

Using the notations of Section 24.1.1 the basic equations in Cartesian coordinates (x,y,z) are:

$$\frac{\partial u}{\partial t} - fv = -g\frac{\partial \zeta}{\partial x} + \frac{\partial}{\partial z}\Big(\nu_T \frac{\partial u}{\partial z}\Big) \tag{24.21}$$

$$\frac{\partial v}{\partial t} + fu = -g\frac{\partial \zeta}{\partial y} + \frac{\partial}{\partial z}\Big(\nu_T \frac{\partial v}{\partial z}\Big) \tag{24.22}$$

$$\frac{\partial T}{\partial t} = \frac{1}{\rho_0 c_p}\frac{\partial I}{\partial z} + \frac{\partial}{\partial z}\Big(\lambda_T \frac{\partial T}{\partial z}\Big) \tag{24.23}$$

where $f = 2\Omega \sin\phi$ is the Coriolis frequency, ϕ the latitude, ζ the surface elevation, T the temperature, c_p the specific heat of seawater at constant pressure and $I(z,t)$ solar irradiance. Neglecting the baroclinic component of the pressure gradient the surface slope terms are written as

$$g\frac{\partial \zeta}{\partial x} = F\cos(\omega_2 t - \varphi_x)\ ,\ g\frac{\partial \zeta}{\partial y} = G\cos(\omega_2 t - \varphi_y) \tag{24.24}$$

where ω_2 is the frequency of the dominant M_2-tide and F, G the specified amplitudes of the surface slope term.

The boundary conditions are

$$\rho_0 \nu_T \Big(\frac{\partial u}{\partial z}, \frac{\partial v}{\partial z}\Big) = (\tau_{s1}, \tau_{s2})\ ,\ \rho_0 c_p \lambda_T \frac{\partial T}{\partial z} = -Q_{nsol} \tag{24.25}$$

at the surface, and

$$\rho_0 \nu_T \Big(\frac{\partial u}{\partial z}, \frac{\partial v}{\partial z}\Big) = \rho_0 C_{db}(u_b^2 + v_b^2)^{1/2}(u_b, v_b)\ ,\ \rho_0 c_p \lambda_T \frac{\partial T}{\partial z} = 0 \tag{24.26}$$

at the bottom where (u_b,v_b) are the velocities at the grid point nearest to the bottom. Different formulations are used for the surface stress and non-solar heat flux Q_{nsol} (see below). The bottom drag coefficient C_{db} is expressed as a function of the roughness length z_0. The solar irradiance in the temperature equation is decomposed into a near-infrared part absorbed in a shallow surface layer, and a non-infrared part which attenuates exponentially within a larger surface layer.

The simulation is performed from the beginning of January until the end of October 1989. As initial temperature the observed vertical profile from the North Sea Project is taken. The meteorological data are obtained from the UK Met Office.

24.2.2 Experiments and output parameters

Nine experiments are defined. The first four (***A, B, C, D***) are intended to examine the role of the turbulence scheme, the next four (***E, F, G, H***) analyse the influence of different heat flux parameterisations at the surface. Light attenuation is disabled in the last experiment ***I***. The general equation of state (4.103)–(4.107) is used in all experiments (iopt_dens=2). Unless stated otherwise all experiments use the setup of reference experiment ***A***.

Table 24.3: Settings of the model switches for the ***csnsp*** experiments. A "-" means that the value of the switch is irrelevant.

switch	***A***	***B***	***C***	***D***	***E***	***F***	***G***	***H***	***I***
iopt_vdif_coef	3	3	3	2	3	3	3	3	3
iopt_turb_alg	-	-	-	2	-	-	-	-	-
iopt_turb_stab_form	3	3	2	-	3	3	3	3	3
iopt_turb_iwlim	1	0	0	-	1	1	1	1	1
iopt_temp_optic	1	1	1	1	1	1	1	1	0
iopt_sflux_cds	6	6	6	6	4	6	5	0	6
iopt_sflux_cehs	0	0	0	0	3	0	4	0	0
iopt_sflux_strat	2	2	2	2	1	0	2	0	2

A **:** Uses the Charnock formulation (4.291) for C_{ds} including Monin-Obukhov stratification (Section 4.8.3). The default turbulence scheme (one equation, $k - \varepsilon$, Blackadar mixing length, Hossain-Rodi RANS model) is taken with limiting condition enabled.

B **:** The limiting conditions for the mixing length and turbulence energy are disabled.

C **:** The formulation (4.199) by Munk-Anderson instead of the RANS formulation (Section 4.4.3.3) is taken for the stability functions and limiting conditions are disabled.

D **:** The turbulence scheme is replaced by the simpler empirical relations (4.136)–(4.140) of Munk and Anderson.

E **:** The surface exchange coefficients C_E and C_H are calculated using the Kondo (1975) formulation (see Section 4.8.2).

F **:** The surface drag coefficient C_{ds} is determined from the Charnock (1955) relation (4.291). C_E and C_H are taken as constants.

G **:** The formulation by Wu (1980) is used with effects of stratification.

H **:** Both surface and heat exchange coefficients are taken as constants.

I **:** The optical mode is disabled, all solar radiation is assumed to be absorbed at the surface.

The values of the model switches, used for setting up each experiment are given in Table 24.3.

The following output parameters are defined:

tsur Surface temperature (°C) measured one-half grid distance below the surface.

tbot Bottom temperature (°C) measured one-half grid distance above the bottom.

tmean Depth-averaged temperature (°C).

tdep The thermocline depth (m) measured as the distance to the surface where the temperature is 1°C higher than the bottom temperature.

tgrad Maximum value of the vertical temperature gradient (°C/m).

twidth This parameter measures the sharpness of the thermocline and is defined as the vertical distance (m) between the two points where the temperature is equal to respectively 8.5 °C and 12 °C.

24.2.3 Results

turbulence schemes Time series of surface and bottom temperature, and mixed layer depth for experiments ***A, B, C, D*** are compared in Figures 24.4a, 24.5a. Vertical profiles on August 4 are shown in Figure 24.6a.

- Surface, bottom and mean temperature are not much different between experiments ***A*** and ***B***. The schemes are almost identical except that the former uses a background mixing scheme based on limiting conditions for turbulence parameters (see Section 4.4.3.6) which results in a deeper thermocline and a less sharper temperature gradient in the thermocline.
- Comparing schemes ***A, C*** and ***D*** it is observed that the first (last two) produce(s) larger (lower) surface temperatures, lower (larger) bottom temperature and larger (lower) temperature gradients in the thermocline. This shows that ***A*** is the least diffusive scheme. This can be explained by the absence of a critical Richardson number for the turbulence schemes used in ***C*** and ***D***.
- The more diffusive scheme ***D*** produces an almost vertically mixed water column at the end of October whereas a significant surface-bottom temperature difference remains in the latter experiments. This is clearly observed in Figure 24.4a.
- Less differences are observed for the depth-mean temperature, although there seems to be a tendency for a higher mean temperature in case of tests ***C, D*** compared to ***A***.
- An additional difference between schemes ***A, B*** and ***C, D*** is that the mixed layer increases smoothly for the former cases whereas

an abrupt increase in mixed layer depth occurs for the latter cases each time the surface temperature drops after a wind event during summer.

drag and exchange coefficients Time series of surface and bottom temperature, mixed layer depth, (upward) non-solar surface heat flux and the exchange coefficient C_E for experiments ***H, A, E, F, G*** are compared in Figures 24.4b, 24.5b and 24.7a–b. Vertical profiles on August 4 are shown in Figure 24.6b.

- The differences between the five experiments are most easily seen in the time series of the surface exchange coefficient. Compared to the reference case ***H*** with constant values and the formulation ***F***, which does not include a dependence on air-sea temperature difference, the C_E coefficient increases by 50% in experiments ***A, G*** and even by 100% (and occasionally 400%) in test ***E***.
- Contrary to what one may expect intuitively, the differences are inversely correlated with the behaviour seen in the evolution of the heat fluxes. For example, experiment ***G*** which shows the lowest time variability for C_E, produces the largest maxima and lowest minima for the heat fluxes. This is explained by a kind of relaxation effect. When C_E increases, the heat flux will first increase as well, so that the air-sea temperature difference is reduced. This occurs quite rapidly and is not seen in the figures showing 3-day averaged values. Once the difference is reduced the heat flux relaxes towards a lower value and C_E rapidly decreases again. If the initial increase of C_E is lower, the time of relaxation becomes longer. This behaviour can be deduced by a close inspection of Figures 24.7.
- Despite the relaxation mechanism, the use of a stratification dependent scheme for the exchange coefficients has an important impact on the evolution of surface temperature in summer by decreasing its value by 2^0C.
- Since all schemes use the same turbulence formulation, the impact on diffusion, thermocline depth and stratification is less.

light attenuation When all solar light is absorbed at the surface itself and no longer within the water column, a strong stratification is produced in a shallow surface layer during periods of strong solar heating and low winds. The result is a damping of turbulence and less downard diffusion, yielding significantly larger surface temperatures (upto 5^0C)

and shallower thermocline as seen in Figures 24.4 and 24.5. The effect on surface temperature is only temporary since the extra surface stratification is removed once the wind increases again.

Results of 1-D numerical simulations at station CS are discussed in Luyten (1996); Warrach (1998).

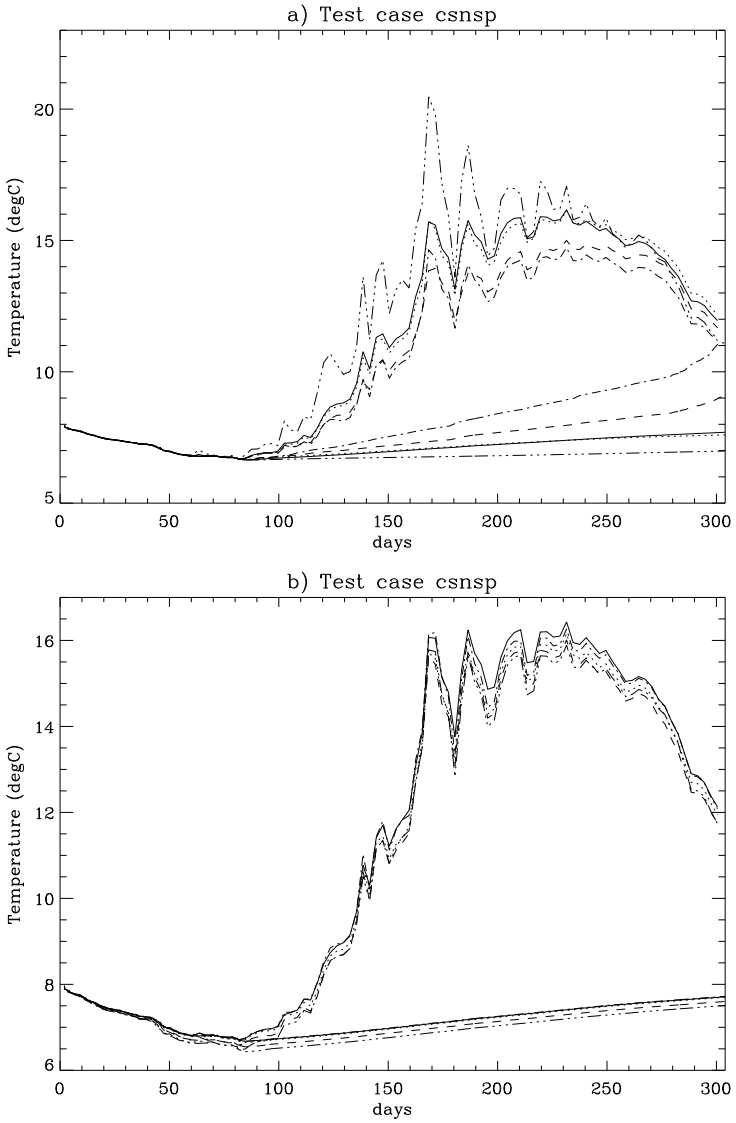

Figure 24.4: Test case ***csnsp***. Time series (3-days average) of surface and bottom temperatures: (a) experiment ***A*** (solid), ***B*** (dots), ***C*** (dashes), ***D*** (dash-dots), ***I*** (dash and 3 dots); (b) experiment ***H*** (solid), ***A*** (dots), ***E*** (dashes), ***F*** (dash-dots), ***G*** (dash and 3 dots).

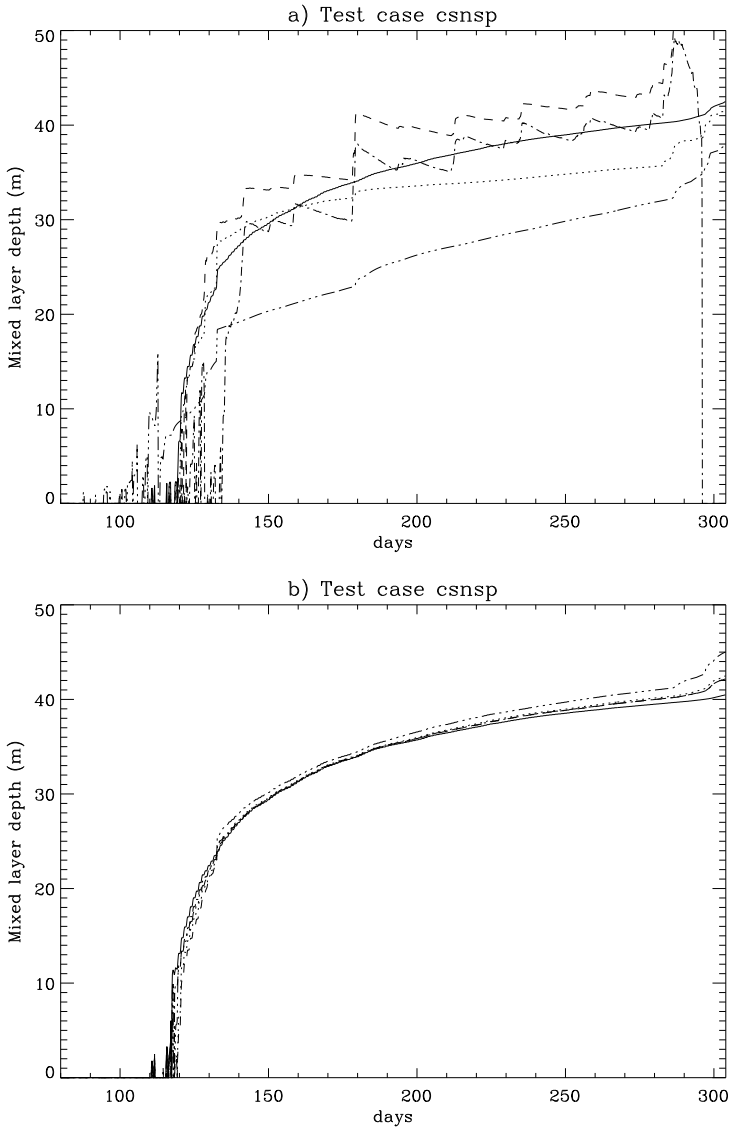

Figure 24.5: Test case ***csnsp***. Time series (3-days average) of mixed layer depth. Legend is as in Figure 24.4.

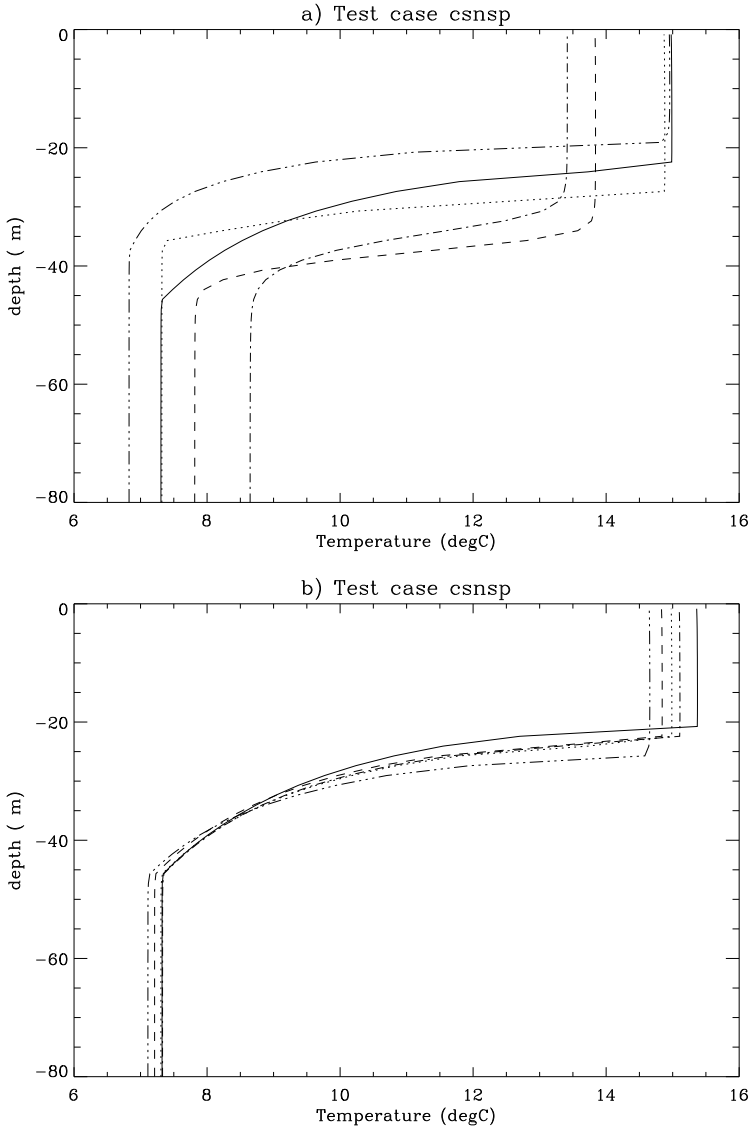

Figure 24.6: Test case ***csnsp***. Temperature profile on August 4. Legend is as in Figure 24.4.

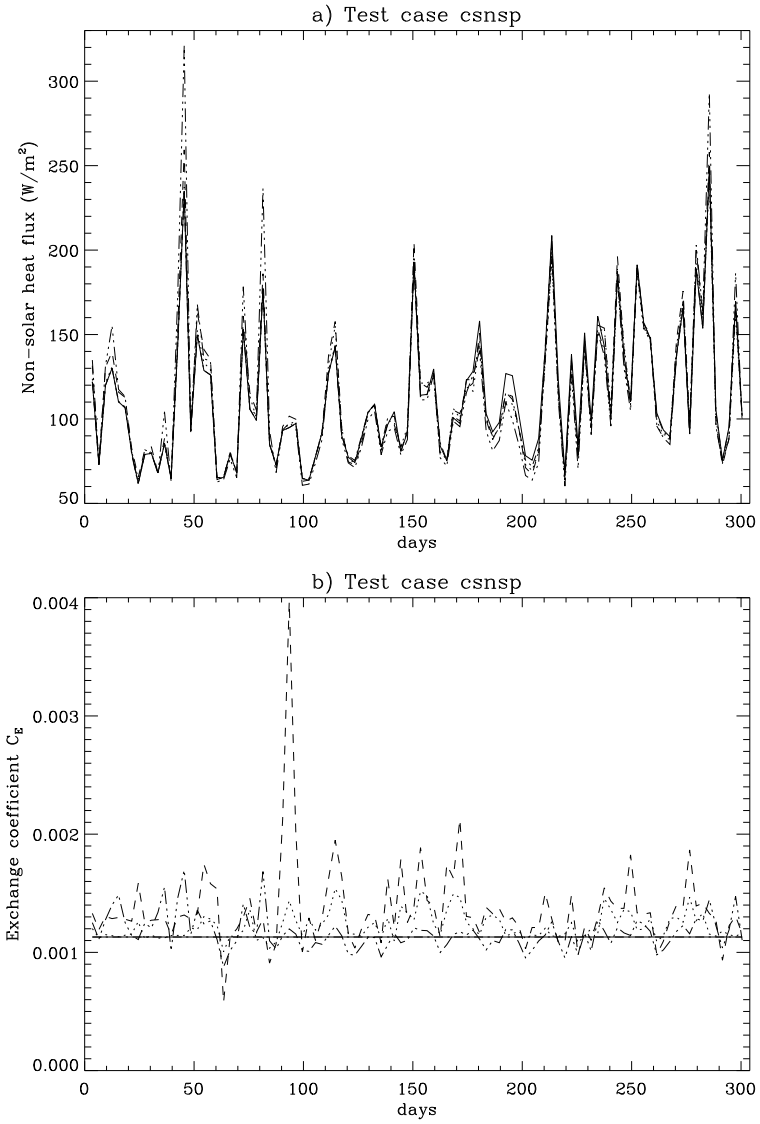

Figure 24.7: Test case ***csnsp***. Time series (3-days average) of (upward) non-solar heat flux (a) and surface exchange coefficient C_E (b) for experiment ***H*** (solid), ***A*** (dots), ***E*** (dashes), ***F*** (dash-dots), ***G*** (dash and 3 dots).